www.czasopisma.pan.pl PAN POLSKA AKADEMIA NAUK www.journals.pan.pl

Arch. Metall. Mater. **67** (2022), 3, 939-948

DOI: https://doi.org/10.24425/amm.2022.139686

K. GOBIVEL[1*], K.S. VIJAY SEKAR[2]

MACHINABILITY STUDIES ON THE TURNING OF MAGNESIUM METAL MATRIX COMPOSITES

Magnesium-based MMCs are widely used in structural-based applications due to their lightweight, high hardness, corrosion and wear resistance. Also, machining is an important manufacturing process that is necessary to ensure dimensional accuracy and produce intricate shapes. In this context, the machining of Magnesium based metal matrix composites is undertaken to study the impact of the cutting parameters on the machinability behaviour. In this work, turning of pure Mg/SiC_p on a Lathe is done and an in-depth assessment on the machining forces, machined surface quality, chip microstructure, and tool morphology has been carried out using TiAlN coated tooling insert. The analysis revealed that the thrust force decreased due to the thermal softening of the matrix meanwhile the feed force also followed the similar trend at higher cutting speeds because of the minimized built-up edge and cutting depth whereas principal cutting force was inconsistent at higher cutting speeds. The surface finish was better at high cutting speed – low feed combination. The chip microstructure revealed that gross fracture propagation at the free surface and variations in the shear bands have occurred at different cutting speeds. Tool studies using SEM analysis revealed wear modes like chipping and built-up edge at low cutting speeds, but with a reduced impact at intermediate cutting conditions, whereas abrasion wear was observed predominantly in the tool nose at higher cutting speeds.

Keywords: Mg-SiC_p composite; cutting forces; surface quality; chip microstructure; tool morphology

1. Introduction

Composite materials are used widely due to their improved wear resistance, higher fatigue life and heat resistance, strength, and stiffness. Mg-based composites possess superior properties such as eco friendliness, light weight, abrasion resistance and non-toxicity which enhances their application in aerospace, automotive and biomedical industries. Even though the composites are preferred to be manufactured near net shape, [1] often machining processes like turning, drilling, milling, etc. are unavoidable in the production of complex designs to attain the required dimensional accuracy, surface finish and functionality [2], despite their high abrasive nature which results in excessive tool wear and higher machining costs.

In the past decade, investigation in machining of aluminium based MMCs has been popular with researchers while magnesium-based composites were hardly studied. Balasubramanian et al. [3] investigated the machinability on LM6/SiC_p MMC, and found that the higher cutting speed, lower cutting depth and moderate feed led to a better surface quality. Samy et al. [4] observed the machining performance during turning of AA6351-B_4C composite and concluded that, at high cutting velocity, the thrust force decreased to protect the tool from abrasion wear and produce better surface quality.

Bai et al. [5] examined the machinability of Al/SiC composites by Ultrasonically Assisted Turning (UAT) which achieved a significant reduction of cutting forces and better surface topography. Suthar and Patel [6] analyzed the influence of machining parameters on aluminium based matrix material and observed that the chips were saw-toothed, discontinuous and serrated. Considerable attention has been given to PCD/CBN ceramic tools for machining hard to cut materials. However, associated costs over these tools are high and therefore PVD coated carbide tools has been used to machine these materials to ensure higher wear resistance, reduce cutting forces and heat generation [7]. At advanced cutting conditions they also provide effective overall machining economy and with their short machining time, rough machining operations can be carried out effectively [8].

Magnesium has a lower density than aluminium which results in superior bonding with reinforcements which reduce the debonding of particles while machining [9]. Ghoreishi et al. [10] evaluated tool wear on the face milling of Al/SiC and observed

[1] KCG COLLEGE OF TECHNOLOGY, KARAPAKKAM, CHENNAI, INDIA
[2] SRI SIVASUBRAMANIYA NADAR COLLEGE OF ENGINEERING, KALAVAKKAM, INDIA
* Corresponding author: gobivel@gmail.com

a significant reduction of wear rates while using cryogenic coolant. Teng et al. [11] studied FEM on micro end milling of Mg based SiC nanoparticles and observed highly stained bands near the particles which caused the lamella structure. A drilling study on Mg/SiC composite was conducted [12] and it was found that adhesive wear was recorded at 4 mm and 6 mm drill tools whereas abrasion wear was found at 8 mm drill tool due to hard reinforcement at low temperature. Reinforcement particle size has influenced the machining output variables on thrust forces, temperature and surface roughness [13].

Balasubramanian et al. [14] discussed the roughness and MRR when machining squeeze cast AZ91D/SiC Mg composites and depicted that a higher percentage of reinforcement leads to a decrease in surface roughness. Brian Davis et al. [15] studied chip formation mechanism on Mg-based MMC by varying different cutting speeds and observed that two kinds of chip morphologies were formed: saw-tooth and discontinuous type chips when cutting speed was less than 0.5 m/s and particle-type chips were found when the cutting speed was greater than 1.0 m/s. Segmented type of chips was observed when Mg/SiC was turned using cryogenic MQL technique [16]. Vijayabhaskar et al. [17] optimized the Wire EDM cutting parameters for nano-based Mg/SiC MMC and showed that the machined surface had craters and cavities due to an increase in pulse time cycle and low vol. (%) of Nano SiC. Abrasive wear was predominant at higher cutting speeds when micro end milling of Tz54 magnesium alloy [18].

Suneesh et al. [19] reviewed the various techniques used to process hybrid-Mg composites and provided insights on tensile and compressive properties, creep and thermal behaviour, hardness and surface aspects related to various reinforcements. Abdulgadir et al. [20] performed a drilling investigation on Mg/SiC/GNPs hybrid composites and observed that maximum thrust force was obtained at low cutting speed and high feed which influenced the surface finish. Gupta and Ling [21] have studied the insights of magnesium composites used in intricate satellite structures, sports applications like tennis racket and golf clubs, automotive parts like gearbox, steering wheel and seat frames. Ramesh et al. [22] reported minimum surface roughness at low cutting speed, 0.1 mm/rev feed and 0.5 mm depth of cut when turning conventional magnesium alloy AZ91D.

Very few studies are available to elucidate the machinability of Mg-based composites. In particular, the effect of cutting speed (v) and feed rate (f) on the machining forces, surface texture, chip microstructure and tool morphology, in turning of Mg/SiC_p Composites are very limited. Hence the focus of the current research is to investigate the machinability of pure Mg/SiC_p MMC using TiAlN coated carbide insert, which would help in the suitable adoption of these materials in building lightweight satellite structures, sporting equipment, machine tools and orthopedic applications.

2. Experimental Work

2.1. Workpiece for experimentation

The matrix selected was magnesium with 99.96% purity and the reinforcement SiC_p with 30 µm was employed for the fabrication using stir casting process as shown in Fig. 1, which is an efficient and cost-effective liquid state technique. Pure magnesium ingot of mass 2 kg was charged into a crucible and its temperature maintained at 700ºC to melt it. Based on the literature, 20-30 vol.% reinforcement are added to increase its hardness and wear resistance property. When considering the stir casting parameters, 20 vol. % chosen to avoid issues with mixing, wettability and difficulty in pouring. To attain a uniform particle distribution, preheating of SiC at 220ºC was done to improve wettability, whereas it is known that Mg content itself increases the wetting property. The preheated SiC was fed into the melt slowly, with the 4-blade stirrer rotated at a constant speed of 500 rpm, which causes a good vortex in the melt and creates better mixing consistency. SEM image showed reasonable consistency in particle distribution across the workpiece and the particle clusters and pores were rarely spotted in certain locations.

The process was completely carried out in an inert environment to avoid explosion of magnesium. The Mg/SiC_p composite

Fig. 1. Stir Casting setup

molten metal was then poured into the mould through the pathway and subsequently squeezed to avoid casting defects. Fig. 2(a) shows the work piece produced as a cylindrical rod of diameter and length 50 mm and 250 mm respectively and Fig. 2(b) shows the microstructure of the matrix and reinforcement. An EDAX was performed to ensure the typical composition of the work material (Fig. 2(c)).

2.2. Machining Tests

The cylindrical rod of Mg/SiC_p MMC was turned on a conventional lathe machine tool (NAGMATI – 175). Fig. 3 shows the experimental methodology carried out in this work. TABLE 1 shows the selected cutting conditions of the machining process. TiAlN PVD coated carbide tool with rake angle of – 6º and clearance angle 6º was mounted on the tool holder (PCLNR 2020 K12) at an inclination angle of 95º. The machining was done at different values of 'v' – 40.52, 61.26, 94.24, 145.14 and 226.19 m/min and 'f' – 0.055, 0.079 and 0.110 mm/rev, at a constant depth of 0.5mm under dry cutting conditions. TiAlN Coated tool provides better thermal insulation, it tends to deflect the cutting heat to the chip and is taken away from the tool due to the presence of an aluminium oxide layer. It also holds its hardness even at a higher temperature where no coolant is used. The range of machining parameters were chosen based on the tool grade, lathe machine power, preliminary experiment trials and available literature data [23-25]. Also, the composite materials are made near net shape, and during fitment only a minimal amount of material needs to be removed which necessitates minimal depth of cut. The KISTLER make (Model 9257 B) piezoelectric dynamometer with the 5070A12100 multichannel charge amplifier, data acquisition system with Dynoware software was used to measure the three-axis cutting forces (F_X, F_Y, F_Z).

To evaluate the machined surface quality the surface roughness 'R_a' was measured using a Mitutoyo make surface

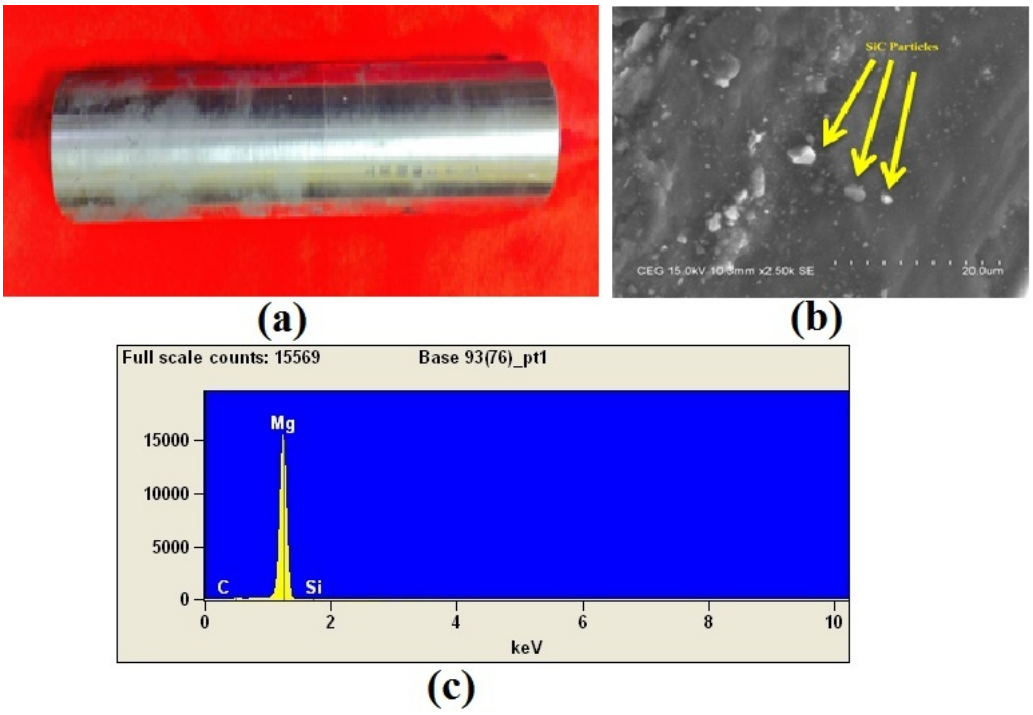

Fig. 2. (a) Fabricated Mg/SiC_p Work piece, (b) microstructure of Mg/SiC_p, (c) EDAX profile of Mg/SiC_p

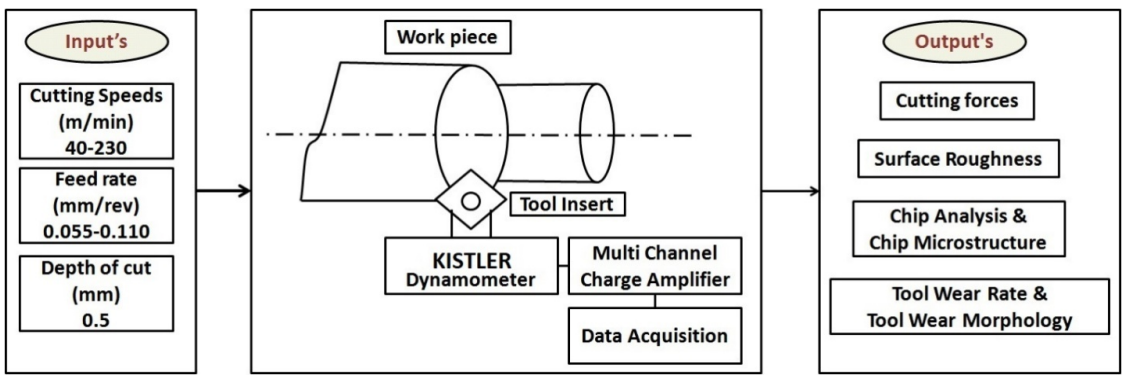

Fig. 3. Experimental methodology

TABLE 1

Experimental Specifications

Factors	Specifications
Work piece dimensions (mm)	50 (OD) X 250 length
SiC vol (%)	20 vol %
Spindle speed 'N' (rpm)	215, 325, 500, 770, 1200
Cutting speed 'v' (m/min)	40.52, 61.26, 94.24, 145.14 & 226.19
Feed rate 'f' (mm/rev)	0.055, 0.079 & 0.110
Depth of cut (mm)	0.5
Environment condition	Dry Condition
Cutting tool	TiAlN Coated Insert (PVD)
Lathe tool dynamometer	Kistler – 9257 B with Data Acquisition
Surface roughness (R_a)	Mitutoyo surftest – SJ 210
Scanning Electron Microscope (SEM) Tool wear (vision measuring system and SEM)	Ion sputter coated with gold target Flank and Crater wear

profilometer surftest (Model SJ-210) with a resolution range of 0.002 µm. The contact stylus tip was moved towards the feed direction for 10 mm distance to measure the 'Ra' with an average of four repetitions on each experimental. The machined chips from each cutting condition were observed using a Scanning Electron Microscope (SEM) and the chip morphology and microstructure were evaluated. The tool flank wear and crater wear were measured with a vision measuring system and the average tool wear width was taken on the flank and rake face to evaluate the actual condition of the tool. For each trial, a new cutting insert was used, and tool wear measurements were taken quantitatively. Average tool wear width was measured on the flank face and rake face of the cutting insert to evaluate the actual condition. The worn cutting tools were also measured by microscopy (SEM) for selected conditions.

3. Results and discussion

3.1. Cutting forces

Fig. 4(a) shows the turning operation on Mg/SiC MMC's and Fig. 4(b), represents the Kistler lathe tool dynamometer and Fig. 4(c), shows the cutting force measurement by data acquisition software. The high compressive contact stress induced by the cutting action of the tool coupled with the frictional stresses results in considerable rise of cutting forces on the tool edge, which is captured in three orthogonal directions, and showed significant variations. Fig. 5(a) depicts the plot of cutting speed versus thrust force (F_X) at different feed rates. At a lower cutting speed of 40.52 m/min and feed rate of 0.059 mm/rev, the maximum thrust force of 173 N was observed and this is the result of stickiness of the magnesium matrix, which has the potential of forming a built-up edge. There is a significant decrease in thrust force when cutting speed increases across feed rates due to the thermal softening of the magnesium matrix, despite the presence of the ceramic particles. The lower thrust force of 72N at high speeds and feeds is the product of the tool impinging on finer particulate reinforcement, with limited abrasion.

The cutting force (F_Y) increased with the cutting speed between 40 to 94 m/min at all feed rates as shown in Fig. 5(b) owing to adhesion at the minor flank. With increasing cutting speed, chip flow extends to the tool nose edge and the chip flows

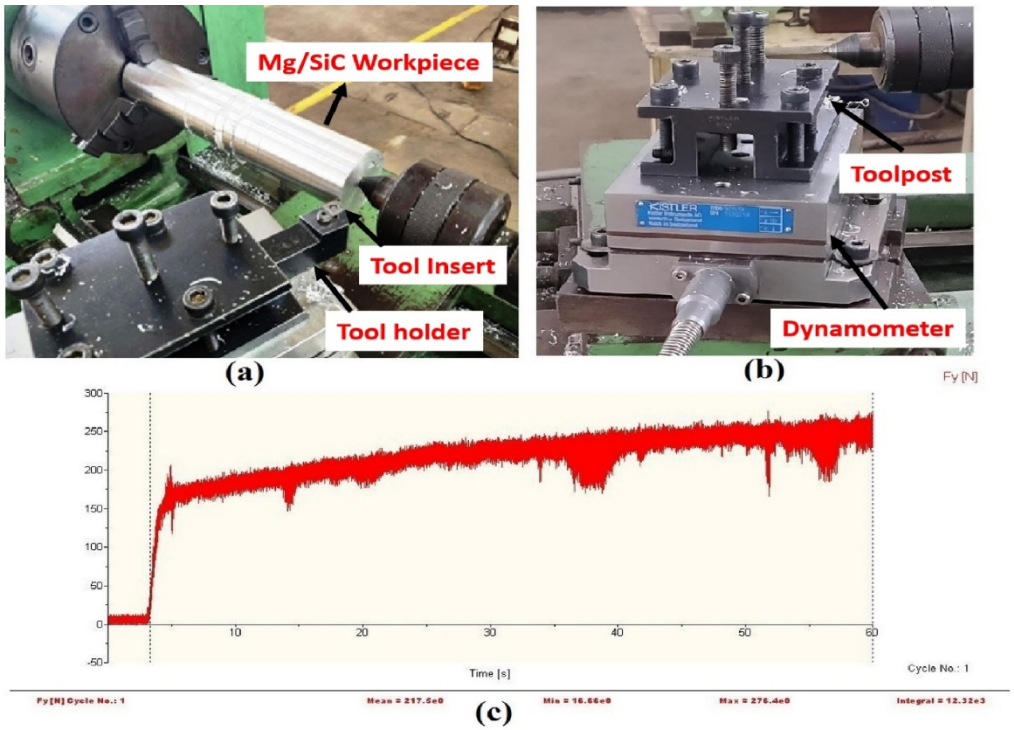

Fig. 4. (a) Machining setup of Mg/SiC_p, (b) Lathe tool dynamometer (c) Cutting force from data acquisition software

towards the rake side of main cutting edge as shown in Fig. 5(d). Higher cutting force magnitude was observed in the Y-direction at low and intermediate feed rates, whereas the cutting force significantly dropped at a feed rate of 0.110 mm/rev because of the larger area around the tool nose radius when compared with the grain size of ceramic particulates, thereby causing particle extrusion along with chip matrix material.

Feed forces 'F_Z' gradually decreased with increasing cutting speeds across all the feed rates due to the minimized built-up edge and cutting depth. At a feed rate of 0.110 mm/rev, the 'F_Z' was lesser in the range of 54 N to 95 N due to better heat conduction between the interfaces of the cutting zone (chip-tool) (Fig. 5(c)).

Thus, the observations showed that thrust and feed forces were impacted by cutting speeds and appeared to be descending owing to the ductile transition despite the presence of particulate reinforcement on Mg matrix. However, the principal cutting force was fluctuating and inconsistent with the increase in 'v'. Meanwhile, at high cutting speeds the cutting force (F_Y) decreased across all the 'f' which showed the good machinability of Mg/SiC_p.

3.2. Surface quality

The R_a was adopted and measured parallel to the feed direction under various turning combinations using Surftest SJ-210 series from Mitutoyo. Fig. 6(a) and 6(b) shows the surface finish (R_a) measured with respect to 'v'and 'f' for the cutting length of 50 mm for all the conditions. The Roughness R_a value decreases with speed across feeds. At low 'v' of 40 and 61 m/min higher surface roughness was reported. Since SiC particulates were pulled out when interacting with the cutting tool, it resulted in pitting which was formed on the finished surface, and this enhances the R_a value. This could be attributed to the fluctuation of cutting forces as shown in Fig. 5(b). Thereafter the roughness value decreases for the cutting speeds 94, 145 and 226 m/min across all the feed rates. After the 'v' of 94 m/min, the surface roughness decreases significantly with decrease in cutting force. At higher 'v', the cutting temperature increases which softens the matrix and aids in the dislocations, thereby reducing the surface roughness.

Fig. 6(b) depicts the plot of surface roughness 'R_a' versus feed rates 'f'. It was observed that increase in 'f' (f = 0.05 & 0.079 mm/rev), causes increase in roughness value significantly. It can be attributed to increase in thrust force which increases the friction leading to poor surface roughness. However, at high 'f', the thrust force was reduced which causes slight changes in roughness values leading to poor machined surface quality. Thus, the combination of high 'v' and low 'f' is recommended to achieve better surface quality while machining Mg-SiC_p composites.

3.3. Chip Morphology

The effect of 'v' and 'f' on chip morphology during turning of Mg/SiC_p composites is shown in Fig. 7. At 'v' 40.52 m/min, the chips were very small, segmented, and in uneven shape with smaller radii C type pattern across the feed rates. The brittle failure becomes more prominent due to the existence of SiC particles

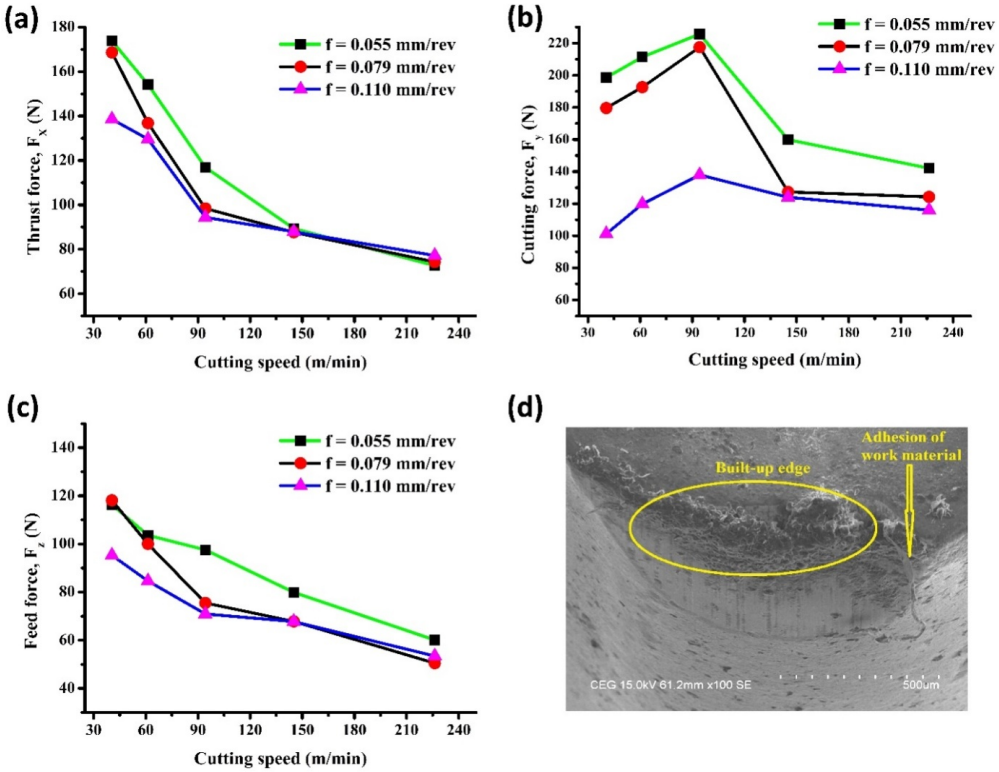

Fig. 5. Effect of cutting speed on forces – (a) Thrust force (F_X), (b) Cutting force (F_Y), (c) Feed force (F_Z), (d) BUE formation on worn tool

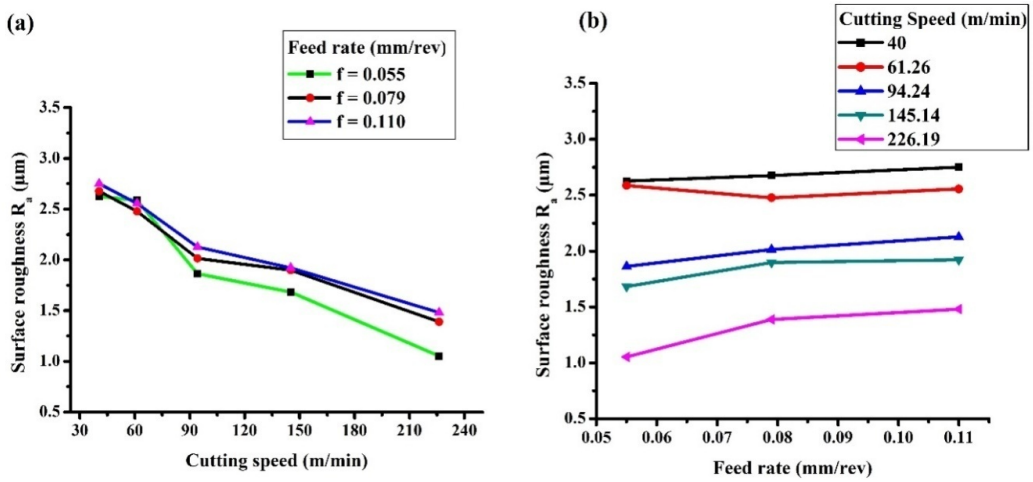

Fig. 6. Surface Roughness R_a – (a) R_a vs 'v' and (b) R_a vs 'f'

while machining of Mg/SiC at lower cutting speed [26]. While turning, the work material undergoes high strain at the shear zones, the particulates are de-bonded, resulting in cracks and the matrix material becomes work hardened, causing short chips.

At the 'v' of 61.26 m/min and 'f' of 0.055 and 0.079 mm/rev the larger radii C type chips were found. At the same 'v' and 'f' of 0.110 mm/rev, continuous and snarled washer type chips were formed. This could be due to the finer particulate reinforcement which tends to stick on the tool surface longer, which leads to continuous curling. Further increasing 'v' to 94.24 m/min generates semi continuous ribbon type chip at low and intermediate feed rates. However, at higher feed rate snarled ribbon chips were found and a similar trend was found at the 'v' of 145.14 m/min. But during higher 'f' with same cutting speed, snarled tubular chips are formed due to the higher tool-chip contact length and higher plastic deformation. High shear strength of the material and reinforcement causes small chips at lower 'v'.

At higher 'v' of 226.19 m/min, semi-continuous snarled tubular chip was observed at low and intermediate 'f' whereas snarled ribbon type formed at higher 'f'. The chip shapes observed in this work are not similar and there was a transition from short-segmented chip to semi-continuous type chip when 'v' goes higher. Thermal softening occurred due to high cutting temperature, which causes local ductility of magnesium and the resulting particle aligns along the shear direction. Thus, based on the range of 'v' and 'f', different types of chips were observed like short flakes, ribbon, semi-continuous, continuous, and tubular types. From the observation of chip morphology, it showed that semicontinuous snarled tubular chip influenced better surface smoothness, which is an indicator of uniform plastic deformation.

3.4. Chip Microstructure

The chips were analyzed using scanning electron microscope to interpret the micro structural changes and deformation behaviour. During low 'v' and 'f', chips produced were highly

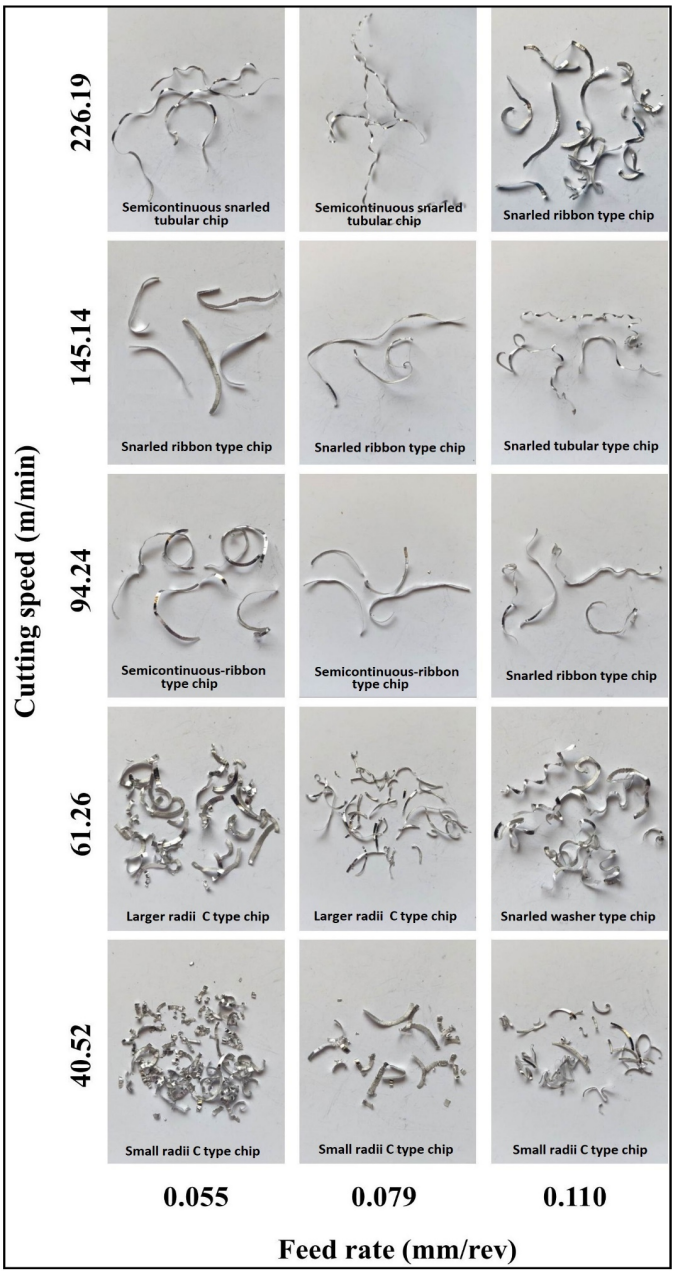

Fig. 7. Effect of cutting speed and feed on chip formation

strained and the particles were pulled out which initiated a crack on the surface of the chip.

Fig. 8(a). shows the crack initiation and subsequent propagation of gross fracture on the chip because of the compressive stress and reinforcement particles in the direction of the shear plane. The larger fracture propagates towards the chip-tool surface at low cutting speeds and feeds while it propagates to one-third or even smaller segment of the chip width at high 'v' and 'f' as shown in Fig. 8(b). Due to thermal softening at high cutting conditions, more compressive stress is not required, so the propagation is limited to smaller distance on the free surface. In Fig. 8(c), it is observed that SiC_p particulate de-bonds and fractures near the shear band edge during low cutting conditions due to higher strain. It is clear that segmentation of shear band depends on the higher concentration of SiC particulates.

Due to the shearing mechanism, the lamella structure is formed which gives irregular and rough appearance on the chip. On closer look at the chip microstructure the lamella structure has two types of orientations – one in which the structure is parallel to a major part of the chip due to side cutting edge and the second which is an inclined lamella on the corner part due to the tool nose edge. At low 'v' and 'f', the lamella thickness is smaller while at higher cutting conditions the thickness is larger. Fig. 8(d) shows the comparison of top surface and back surface topography where the back surfaces of the chips are smooth despite encountering the combined effects of high friction and temperature.

During machining of Mg/SiC_p, saw tooth edges were observed prominently on the outer surface, and the shear bands were seen in all the cutting conditions. The geometrical characteristics of chip segmentation varied based upon different 'v' and 'f'. The important characteristics of chip segmentation are saw tooth spacing distance, shear band spacing, shear plane length, inclination angle and shear band [27]. Fig. 9(a-e) shows the longitudinal cross section of chip segments taken in SEM at different 'v' and 'f'. It was observed that the saw tooth space distance decreased with increasing cutting speed due to reduced plastic deformation and high temperature and the same trend was observed for the entire shear plane length where the length decreases at high 'v' as shown in Fig. 9(d-e).

3.5. Tool Morphology

Distinctive tool wear morphology of TiAlN cutting tool after dry turning of Mg/SiC MMC is shown in Fig. 10(a-c). At low 'v' from 61 to 94 m/min, the magnesium matrix becomes soft and sticky towards the tool edge resulting in BUE which prevents the cutting edge from abrasion, but leads to instability, inducing tool chipping and causing poor surface as shown in Fig. 10(a). Formation of BUE has been measured using scanning electron microscope to study its impact on cutting edge. The main causes for chipping are the combined effect of impact stresses and stress concentration. At higher 'v' abrasion wear was found predominantly at the tool nose and flank face due to the fluctuation in 'F_Y' on the cutting edge because of the reinforced particles which is harder to grind. At higher feed rates the sharp edges of pulled out SiC particles fall on the tool nose and flank face and results in slight abrasion. Also, it is found that uniform

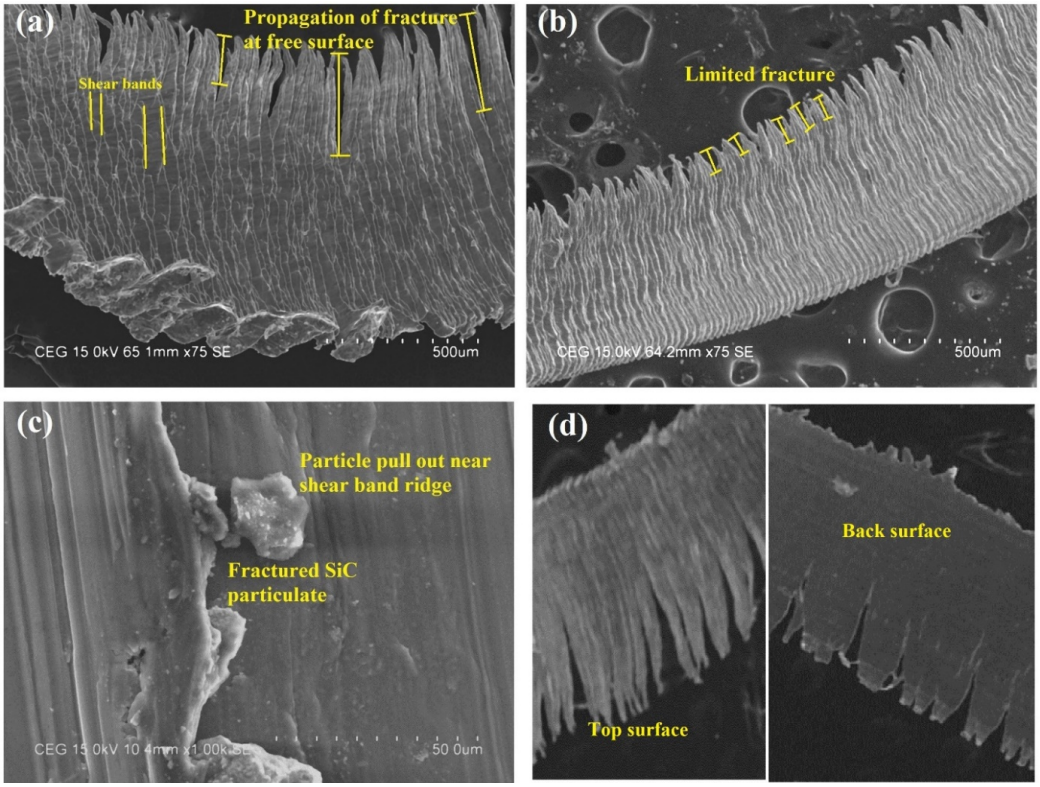

Fig. 8. Crack propagation at (a) 'v' 40.52 m/min, 'f' 0.110 mm/rev, (b) 'v' 226.19 m/min, 'f' 0.110 mm/rev, (c) Fracture at 'v' 40.52 m/min, 'f' 0.110 mm/rev and (d) Top and back surface topography of the chip

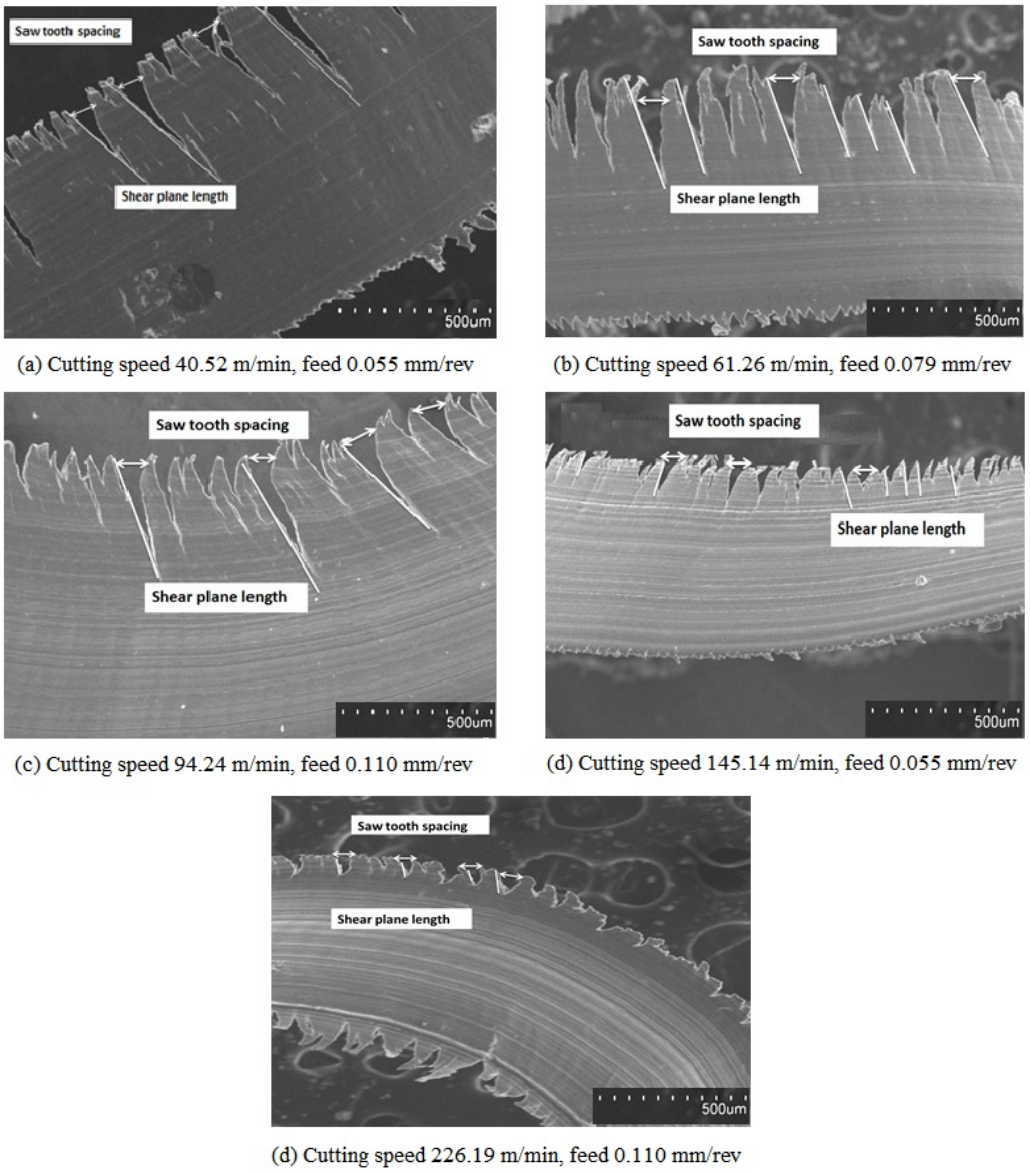

Fig. 9. Combined effects of cutting speed and feed on-chip segmentation

and closely packed flank wear which can be attributed to the evenness of the coating of TiAlN on the carbide insert.

The flank wear was noted using a vision measurement system and it was found to be 0.86 mm, at higher 'v' and 'f' and a minimum of 0.32 mm at 61.26 m/min. Increasing the 'f' causes an increase in the wear rate. Flank wear of 0.48 mm was observed at a 'f' of 0.077 mm/rev, which is considered as an optimum feed to improve the tool life. Grooves were found on the worn flank face as shown in Fig. 10 (b), due to slight abrasions between cutting tool and reinforcement particle [28] while turning Mg/SiC metal matrix composites at 'v' of 145.14 m/min and 'f' of 0.079 mm/rev. Since the reinforced particles are harder, they are sheared and also result in a random micro-cut at the tool edge.

Crater wear was measured on the turning tool and exhibited in Fig. 10(c). Due to the combined effect of a high compressive stress and a sliding effect of the chip at high temperature over the tool rake, crater wear occurs. At low 'v' of 40m/min and 'f' of 0.055 mm/rev the extent of crater wear formed on the tool rake face is less. When the 'v' and 'f' increases, crater wear also increases on the top rake face due to the flow of semi-continuous chips on the interface. The maximum crater wear of 0.43 mm was noted at a 'v' of 226.19 m/min and 'f' of 0.110 mm/rev.

4. Conclusions

Mg-SiC_p particulate MMC work piece has been machined using TiAlN cutting tool under different 'v' and 'f' at constant depth and a systematic assessment on the cutting forces, surface quality, chip microstructure and tool morphology has been reported.

- The cutting speed had a significant influence on all three cutting forces, where forces decreased when cutting speed increased. However, the principal cutting force was increased from 40 to 94 m/min and then decreases significantly at 145

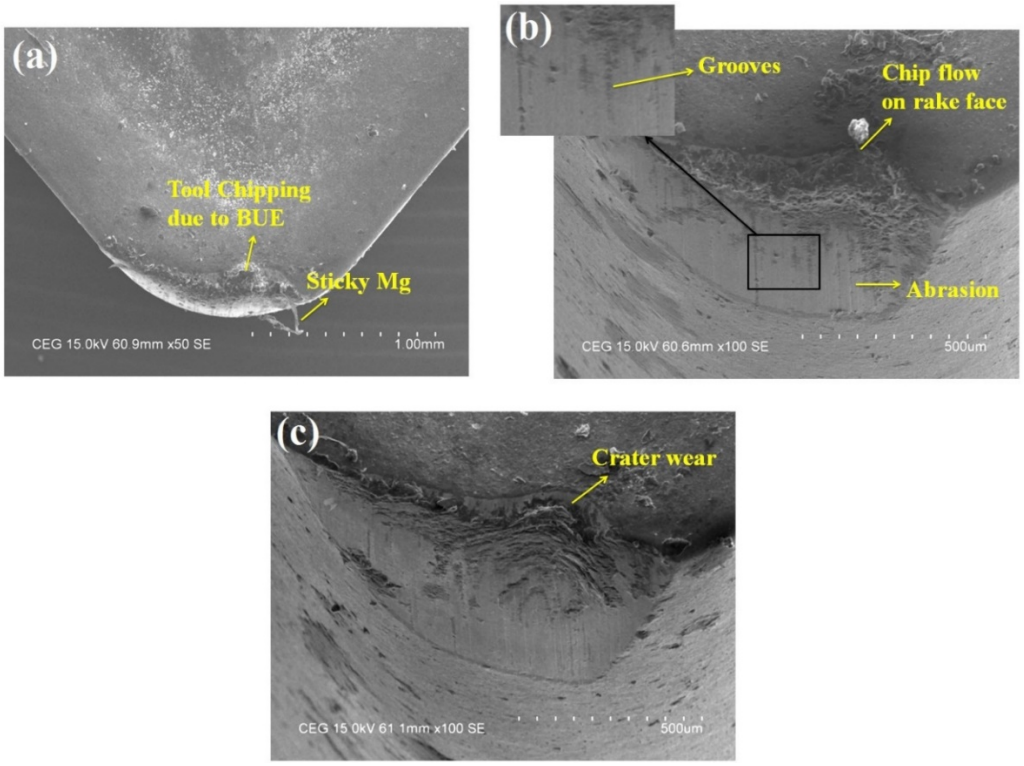

Fig. 10. Worn tool (a) Crater wear at 'v' 61.26 m/min, 'f' 0.055 mm/rev, (b) Flank wear at 'v' 145.14 m/min, 'f' 0.079 mm/rev and (c) Crater wear at 'v' 226.19 m/min, 'f' 0.110 mm/rev

and 226 m/min. The feed force and thrust force decreases with increase in cutting speed because of ductile transitions, despite the presence of SiC particulates.

- Built-up edge generated leads to the cause of increase in cutting force at low cutting speed. Crater wear, tool chipping, flank wear and abrasion mechanisms dominated the wear modes. An optimal 'v' of 60-94 m/min and 'f' of 0.055-0.088 mm/rev is necessary to balance the machining integrity and results in higher tool life.
- At low 'v' of 40-60 m/min short-flakes, ribbon type and segmented type chip was formed, whereas at intermediate and high 'v' of 90-226 m/min, semi-continuous, tubular type and continuous chips were observed. Saw toothed profile produced during machining of Mg/SiC_p showed significant variation with respect to increase in 'v'.
- The 'v' and 'f' showed equal influences on the average roughness (R_a) characteristics. The optimum condition of high 'v' and low 'f' with 0.5 mm depth of cut is suggested for achieving better surface quality.
- In summary it is recommended that a high cutting speed 226 m/min and low feed rate of 0.055 mm/rev can be utilized for the optimum results when turning Mg/SiC_p composite to attain an optimum machining output.

REFERENCES

[1] J.Y. Sheikh-Ahmad, Machining of polymer composites, Springer, New York (2009).

[2] Y. Allwin Roy, K. Gobivel, K.S. Vijay Sekar, S. Suresh Kumar, Arch. Metall. Mater. **62** (3), 1771-1777 (2017). DOI: https://doi.org/10.1515/amm-2017-0269

[3] K. Balasubramanian, M. Nataraj, P. Duraisamy, Mater. Manuf. Process. **34** (12), 1389-1400 (2019). DOI: https://doi.org/10.1080/10426914.2019.1660787

[4] G.S. Samy, S. Thirumalai Kumaran, M. Uthayakumar, J. Test. Eval. **49** (3), (2019). DOI: https://doi.org/10.1520/JTE20180429

[5] W. Bai, A. Roy, R. Sun, V.V. Silberschmidt, J. Mater. Process. Technol. **268**, 149-161 (2019). DOI: https://doi.org/10.1016/j.jmatprotec.2019.01.017

[6] J. Suthar, K.M. Patel, Mater. Manuf. Process. **33** (5), 499-527 (2018). DOI: https://doi.org/10.1080/10426914.2017.1401713

[7] Y. Sahin, G. Sur, Surf. Coatings Technol. **179**, 349-355 (2004). DOI: https://doi.org/10.1016/S0257-8972(03)00802-8

[8] R. Teti, CIRP Ann. – Manuf. Technol. **51** (2), 611-634 (2002). DOI: https://doi.org/10.1016/S0007-8506(07)61703-X

[9] J. Paulo Davim, Machining of Metal Matrix Composites, Springer, London (2012).

[10] R. Ghoreishi, A.H. Roohi, A.D. Ghadikolaei, J. Brazilian Soc. Mech. Sci. Eng. **41**, 416 (2019). DOI: https://doi.org/10.1007/s40430-019-1649-3

[11] X. Teng, D. Huo, W. Chen, E. Wong, L. Zheng, I. J. Manuf. Process. **32**, 116-126 (2018). DOI: https://doi.org/10.1016/j.jmapro.2018.02.006

[12] K. Balamurugan, M. Uthayakumar, S. Thirumalai Kumaran, G.S. Samy, U.T. S. Pillai, Def. Technol. **15**, 557-564 (2019). DOI: https://doi.org/10.1016/j.dt.2019.01.002

[13] P.M. Gopal, K. Soorya Prakash, S. Ramesh Kumar, Silicon. 1-11 (2020). DOI: https://doi.org/10.1007/s12633-020-00749-y

[14] I. Balasubramanian, R. Maheswaran, V. Manikandan, N. Patil, M.A. Raja, R.M. Singari, Procedia Manuf. **20**, 97-105 (2018). DOI: https://doi.org/10.1016/j.promfg.2018.02.014

[15] B. Davis, D. Dabrow, L. Ju, A. Li, C. Xu, Y. Huang, J. Manuf. Sci. Eng. Trans. ASME, **139**, 1-10 (2017). DOI: https://doi.org/10.1115/1.4037182

[16] N. Khanna, P. Shah, N.M. Suri, C. Agarwal, S.K. Khatkar, F. Pusavec, M. Sarikaya, Silicon. 1-15 (2020). DOI: https://doi.org/10.1007/s12633-020-00588-x

[17] S. Vijayabhaskar, T. Rajmohan, Silicon, **11**, 1701-1716 (2019). DOI: https://doi.org/10.1007/s12633-017-9676-0

[18] A. Ercetin, K. Aslantas, O. Ozgun, Mach. Sci. Technol. **24** (6), 924-947 (2020). DOI: https://doi.org/10.1080/10910344.2020.1771572

[19] E. Suneesh, M. Sivapragash, Mater. Manuf. Process. **33** (12), 1324-1345 (2018). DOI: https://doi.org/10.1080/10426914.2018.1453155.

[20] M.M. Abdulgadir, B. Demir, M.E. Turan, Metals **8** (4), 1-14 (2018). DOI: https://doi.org/10.3390/met8040215

[21] Manoj Gupta, Nai Mui Ling Sharon, Magnesium, Magnesium Alloys and Magnesium Composites, John Wiley, New Jersy (2011).

[22] S. Ramesh, R. Viswanathan, S. Ambika, Measurement **78**, 63-72 (2016). DOI: https://doi.org/10.1016/j.measurement.2015.09.036

[23] C.J. Nicholls, B. Boswell, I.J. Davies, M.N. Islam, Int. J. Adv. Manuf. Technol. **90**, 2429-2441 (2017). DOI: https://doi.org/10.1007/s00170-016-9558-4

[24] S. Gururaja, M. Ramulu, W. Pedersen, Mach. Sci. Technol. **17**, 41-73 (2013). DOI: https://doi.org/10.1080/10910344.2012.747897

[25] S. Chinchanikar, S.K. Choudhury, Int. J. Refract. Met. Hard Mater. **38**, 124-133 (2013). DOI: https://doi.org/10.1016/j.ijrmhm.2013.01.013

[26] U.A. Dabade, S.S. Joshi, J. Mater. Process. Technol. **209** (10), 4704-4710 (2009). DOI: https://doi.org/10.1016/j.jmatprotec.2008.10.057

[27] S. Zhang, Y.B. Guo, Int. J. Mach. Tools Manuf. **49** (11), 805-813 (2009). DOI: https://doi.org/10.1016/j.ijmachtools.2009.06.006

[28] I. Ciftci, M. Turker, U. Seker, Mater. Des. **25** (3), 251-255 (2004). DOI: https://doi.org/10.1016/j.matdes.2003.09.019